Millimeter-Wave Fiber Optics Systems for Personal Radio Communication

Hiroyo Ogawa, *Member, IEEE,* David Polifko, *Member, IEEE,* and Seiichi Banba

***Abstract*—System concepts for millimeter-wave personal communication systems and the advantages of millimeter-wave band usage are briefly described. Demonstration of broad-band millimeter-wave subcarrier transmission concepts over fiber optic links is performed. Several fiber optic link architectures, including one using a combination of direct laser modulation and indirect (external) optical modulation, are outlined with respect to signal transmission at millimeter-wave frequencies. Several configurations are experimentally investigated using 70 MHz, 300 MHz and 26 GHz subcarriers which transmit either FM or QPSK data signals. Additionally, the use of optical MMIC technology, which can result in the design of compact and cost-effective optical receivers, is described with respect to personal communication radio base station equipment. MMIC HEMTs operating as photodetectors are newly characterized in terms of digital and analog signal reception with excellent performance being observed.**

Introduction

FIBER OPTIC signal feeds in microcellular radio systems have been investigated for mobile and personal communication systems [1]–[6]. Because the average cell is usually less than several hundred meters in diameter, a large number of remote radio base stations (cells) are required for effective signal distribution over a given area. Therefore, it is important to develop cost-effective technology for miniaturized radio base stations and the signal distribution paths which will feed into them. Typically, each base station consists of a transceiver module, containing electrooptic and optoelectric converters and related electrical components, as well as an optical link to connect it to the central base station. Similar systems have been demonstrated using UHF-band subcarrier frequencies (radio frequencies or RF) which are transmitted via optical fiber and then subsequently propagated within the microcell zone. Commercially available optical devices have been successfully utilized to demonstrate these low frequency fiber optic microcellular mobile systems [2], [5]. However, broadband distribution, such as FM video signals, at millimeter-wave frequencies has not yet been realized within the above system configuration.

In this work, millimeter-wave subcarrier transmission by fiber optic links is investigated for the purpose of supplying broadband signals to a large number of personal communication terminals. Broadband video distribution networks have been previously demonstrated using subcarrier multiplexing techniques which utilize the advantages of fiber optic links, e.g. low transmission loss and potential bandwidth [7]–[10]. Conversely, in several radio transmission systems, millimeter-wave distribution networks have been investigated for video signal transmission [11]–[12]. In these cases, the millimeter bands are very attractive in terms of large bandwidth and short frequency reuse distances. In our proposed radio distribution systems composed of fiber optic millimeter-wave subcarrier transmission links, we exploit the advantages of both optical fibers and millimeter-wave frequencies to service broadband communication systems. Several fiber optic link configurations are characterized for transmission of analog video signals as well as digital data signals.

Another key issue to realizing personal millimeter-wave radio systems is the development of compact and cost-effective radio base station hardware. Monolithic microwave integrated circuit (MMIC) technology has the potential to reduce both size and cost of electrical transceivers [13]. However, personal communications systems require an interface between the optical signals and RF signals to and from the mobile personal terminals. Although the concurrent use of MMICs and discrete optical devices is one solution for this interface, such hybrid integrated circuit (HIC) technologies have cost, size and performance limitations due to the essential differences between the MMIC and discrete device fabrication processes [14]. Optoelectronic integrated circuit (OEIC) technology is another alternative for inexpensive hardware. However, despite many potential advantages of monolithic integration, OEICs have yet to outperform HICs because of their complicated fabrication process and inherent circuit limitations [15]. MMIC compatible optical device technology is still the best alternative to configure monolithic transducer modules [16]–[17]. MMIC-type photodetectors are currently integratable with microwave circuitry using a standard MMIC fabrication processes [18]. This paper demonstrates millimeter-wave subcarrier data signal transmission for the first time using custom fabricated MMIC HEMT optical detector circuits.

Transmission characteristics of the fiber optic links are evaluated using both 0.83 μm and 1.3 μm wavelength optical carriers which are intensity modulated by either 70 MHz and 26 GHz band QPSK modulated subcarriers or 300 MHz and 26 GHz band FM modulated subcarriers.

Manuscript received March 31, 1991; revised July 27, 1992.
The authors are with ATR Optical and Radio Communications Research Laboratories, 2-2 Hikaridai, Seika-cho, Soraku-gun, Kyoto 619-02, Japan.
IEEE Log Number 9203705.

0018-9480/92$03.00 © 1992 IEEE

The HEMT optical detectors are characterized within a 0.83 μm optical carrier system and are then compared with the experimental results of devices operating at 1.3 μm.

Millimeter-Wave Fiber Optic Feed Concept

The system concept of the fiber optic millimeter-wave subcarrier transmission link is shown in Fig. 1. A large number of modulated millimeter-wave subcarriers are combined electrically by power combiners. The optical carrier is intensity modulated by this composite signal, transmitted by single-mode fiber, and is then optically divided at each radio base station. The tapped optical signal is directly detected by a high-frequency photodetector and amplified by MMIC amplifiers. The amplified millimeter-wave signals are subsequently radiated into the microcell zone (down link) and received by portable communication terminals.

Each radio base station also receives millimeter-wave signals from the portable terminals and down-converts them to RFs by using a frequency converter and local oscillator signal. The down-converted signals are used to intensity modulate a relatively inexpensive and low frequency laser diode. The optical signals from each radio base station are combined and then transmitted back to the central base station over singlemode fiber. The received optical signals are detected, amplified and demultiplexed (up link).

Because of the site-specific location of each radio base stations (e.g., light posts, telephone boxes, sides of buildings, etc.) they must be small and should broadcast over limited (less than several 100 meters) and well defined areas (within a city block or within one floor of a building for example). To avoid frequency interference between adjacent zones, different millimeter-wave subcarrier frequencies are utilized within two adjacent zone. Simultaneous use of fiber optic distribution links and millimeter-wave frequencies provide the following advantages within microcellular systems:

1) Fiber optic transmission lines have practically zero loss for lengths less than one kilometer. Thus cell spacing is limited only by the millimeter-wave radio signal transmission range, propagation effects such as multipath fading, and attenuation due to rain. Additionally, the technology for fiber optic communication is maturing to the point of being financially and technologically competitive with all electrical broadcast systems.

2) Millimeter-waves are essentially broadband frequencies which can transmit a large number of video/voice subcarriers. For example, an FM-modulated 4.2 MHz NTSC video signal requires a 36 MHz transmission bandwidth [19]. If the channel separation is 40 MHz [7] with 100 channels being transmitted, the resultant radio frequency bandwidth is 4 GHz. At a 60 GHz subcarrier frequency, the relative bandwidth is only 7 percent.

3) Millimeter-waves are readily absorbed by oxygen and water molecules [20]. At 60 GHz there is an absorption peak (16 dB/km) due to atmospheric oxygen. At a transmission frequency of 60 GHz for example, this absorption effect can be selectively exploited to limit signal propagation beyond the microcell boundaries. However, local regulations governing frequency usage need to also be considered in choosing subcarrier frequencies in the final system implementation.

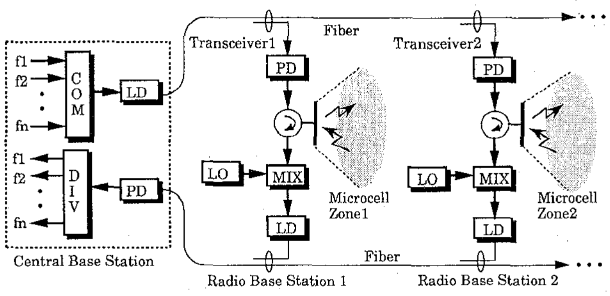

Fig. 1. Conceptual diagram of fiber optic millimeter-wave subcarrier transmission link system.

4) The system control functions, such as frequency allocation and a modulation/demodulation scheme, can be located within the central base station. This simplifies the design of the radio base station, more so if the subcarrier frequency is distributed from the central base station. The primary functions of the radio base stations are optical/RF conversion, RF amplification, RF down conversion, and RF/optical conversion. Because all of the components required for these functions are analog devices, monolithic integration technologies can be adopted to configure radio base station hardware.

Link Configurations

Millimeter-wave signal transmission over fiber optic links has been attempted using external modulators, indirect subharmonic injection-locking techniques, laser diode nonlinearity [21], photodiode nonlinearity [22] and heterodyne techniques [23]. The laser diode's fundamental modulation response is limited to frequencies below its relaxation oscillation frequency (typically <20 GHz for high-speed commercial devices). Conversely, external optical modulators, such as $LiNbO_3$ integrated devices, are capable of modulation into the millimeter-wave bands despite their typically high driving voltages and optical insertion losses [24]. In this work, we combine both the advantages of direct laser diode modulation and $LiNbO_3$ external modulation to develop a unique fiber optic link architecture suitable for economical millimeter-wave subcarrier transmissions.

Several fiber optic down-link configurations (i.e., the link from the central base station to the radio base station) are shown in Fig. 2. The fiber optic up-link from the radio base station to the central base station is shown conceptually in Fig. 3. In all of these fiber optic links, the low frequency data (or control) signals are transmitted by conventional direct laser diode current modulation [25]. Technology for directly modulated laser links is well developed and can provide substantial benefits over external modulation techniques at low frequencies. These advantages include potentially higher link gain, reduced num-

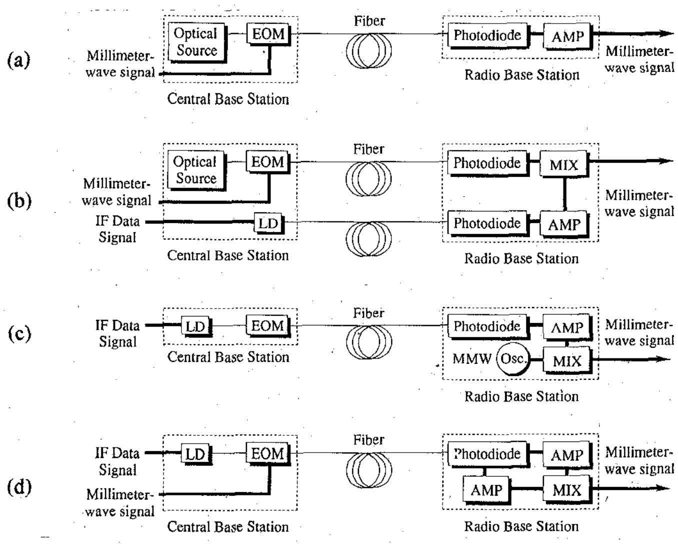

Fig. 2. Fiber optic link architectures for millimeter-wave subcarrier transmission: Down-link from central base station to radio base station. (a) Millimeter-wave external modulation transmission link A. (b) Dual-fiber millimeter-wave transmission link B. (c) Remote millimeter-wave transmission link C. (d) Dual-modulation millimeter-wave transmission link D.

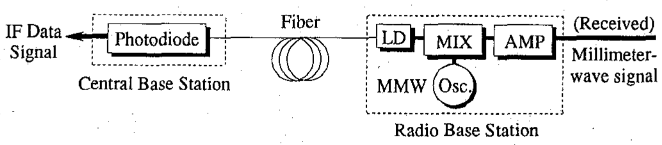

Fig. 3. Fiber Optic up-link from radio base station to central base station. Low frequency lasers and photodiodes are utilized. MMW oscillator signal can be obtained from central base station.

ber of components and reduced system cost when the link is specifically optimized for a particular frequency and bandwidth [27].

The millimeter-wave subcarrier frequency is optically generated by using an external optical modulator such as a Mach–Zehnder interferometer realized in $LiNbO_3$, or by using a local oscillator in the radio base station as in Fig. 2(c). Generating the millimeter-wave subcarrier in the central base station however, reduces the overall cost and complexity of the radio base stations as well as centralizes the local oscillators. Because the bandwidth of the laser diodes does not currently extend into the millimeter-wave band, EOMs are the most simple and cost-effective devices for providing these subcarrier frequencies.

Although the conventional link architecture shown in Fig. 2(a) is the simplest to implement, the high link insertion loss can sometimes deteriorate multiplexed millimeter-wave signals [26]. The architecture shown in Fig. 2(b) improves the performance of the overall system by optimizing the two separate links. Unfortunately, separating the subcarrier and the data signals results in an increase in components, complexity and cost. This is an unwelcome characteristic in systems as diverse as multicellular signal distribution.

A beneficial compromise between performance and system complexity is presented in Fig. 2(d). This architecture combines the simplicity of single laser/fiber/detector transmission in addition to preserving the performance at the millimeter-wave subcarrier frequencies. Although there is additional loss in the laser generated data signal due to the EOM insertion loss, this should not translate into a significant deterioration in fidelity if high output power laser diodes are utilized for the EOM optical source. Commercial laser diodes with modulation bandwidths up to 5 GHz can typically have >5 mW output power, which is comparable to solidstate lasers that can be used in EOM driven links. Thus, only one optical source is required to produce a data and subcarrier-frequency modulated optical carrier for an economical and compact optical transmitter.

In the link architecture of Fig. 2(d), the EOM is a key component for realizing millimeter-wave transmission. Within this configuration, the data signal can be used to modulate the laser diode, while a single frequency subcarrier can modulate the EOM. In this situation, the EOM need not operate over a substantial bandwidth, thus simplifying its design. Conversely, in the case where the subcarrier multiplexed data directly modulates the EOM, the EOM design becomes more complex, considering the required bandwidth for successful data transmission. However, the laser can still be modulated with control signals for use in communicating with each of the base stations. We are currently investigating the processes for accurate design of millimeter-wave EOMs [35].

The up-link architectural configuration is shown in Fig. 3. Conventional microwave heterodyne techniques are adopted at the radio base station for simplicity. The received millimeter-wave signals are down-converted to IF signals by the frequency mixer. The local oscillator signal can be supplied by the down-link through filtering and amplification. After amplification of the down-converted IF data signals, these signals modulate a low bandwidth laser diode and are subsequently transmitted to the central base station through singlemode optical fiber. All of the up-link RF components, except for the laser diode, can be monolithically integrated using the MMIC process, thus reducing the size and potential cost of the radio base station.

HEMT Photodetection

MESFETs and HEMTs have received much attention for realization of photodetector functions [29]–[31]. The monolithic integration of optical and microwave/millimeter-wave circuits has great potential reducing the complexity of optical front ends for millimeter-wave systems [28], [32]. That which displays the greatest potential is the photodetection function. The optimization of MMIC active devices requires few alterations for optical operation.

To demonstrate the principles of monolithic integration of optical and microwave/millimeter-wave circuits and to demonstrate their performance in optical receivers, custom MMIC circuits are designed around Mitsubishi processed n-AlGaAs/InGaAs HEMTs [36]. The HEMTs are designed for 0.83 μm wavelength photodetection and have

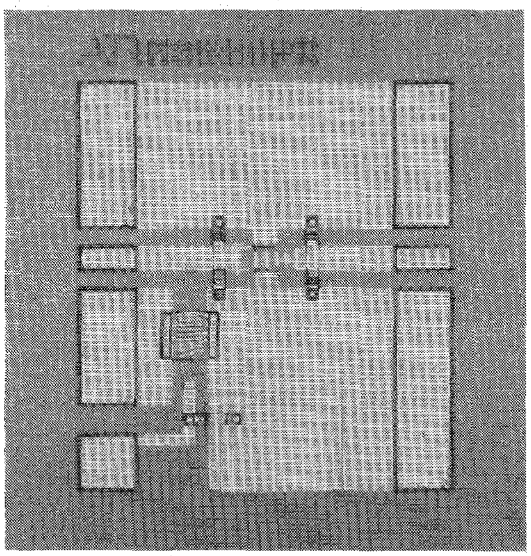

Fig. 4. Micro-photograph of ATR designed circuit with common source HEMT photodetector fabricated on a GaAs substrate.

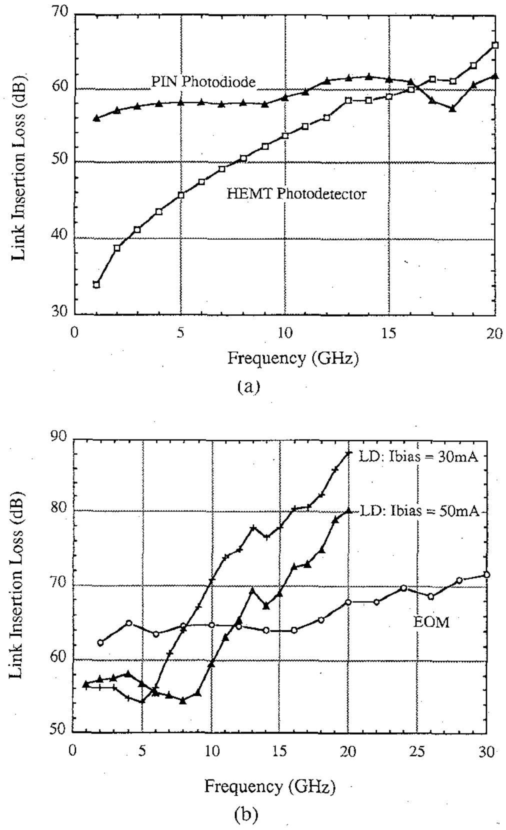

Fig. 5. Fiber optic link insertion loss versus frequency using both external and direct modulation. (a) 0.83 μm PIN photodiode and MMIC HEMT photodetector. (b) 1.3 μm laser diodes, external optical modulator and PIN photodiode.

a cutoff frequency of approximately 40 GHz, gate length of 0.25 μm, and gate width of 100 μm. A photograph of common source HEMT photodetector circuit fabricated on a GaAs substrate is shown in Fig. 4. The relative frequency response of the HEMT photodetector is graphed along with a PIN photodiode (which includes a 50 Ohm matching resistor), both with identical optical transmitters, in Fig. 5(a). At zero gate bias, the HEMT has an optical dc responsivity of 2.1 mA/mW. The ultra-wideband PIN photodiode (New Focus 1001) has 3-dB bandwidth and responsivity of 40 GHz and 0.52 mA/mW, respectively.

A $LiNbO_3$ external modulator is used as the optical transmitter. Optical insertion loss is 9 dB and the voltage, $V\pi$, for 100% modulation is 2.3 V. The optical power is delivered to each detector via a single mode fiber with a spot diameter less of than 10 μm in the case of the HEMT. Link insertion loss is significantly improved at lower frequencies with the HEMT photodetector because of the device's internal gain. However, the advantages of using the HEMT photodetector, based on frequency response alone, are soon outweighed by the flat response of the PIN diode after 15 GHz. Additionally, as will be seen in the BER measurements, the noise floor of the HEMT link is substantially higher than that of the PIN diode. Therefore, at this time there is not a particularly significant improvement in the link dynamic range for higher frequency bands.

In order to improve the performance of the HEMT as a photodetector, increasing the optical coupling, improving the electrical characteristics and using impedance matching techniques will all prove to be beneficial. Additionally, a longer optical wavelength could be used as a carrier by choosing a different device material such as InP [15]. Again, the primary benefit of HEMT usage will come from the ability to monolithically integrate these type of detectors within other millimeter-wave circuitry as well the potential for improved performance as this technology matures.

Fiber Optic Link Frequency Response

The fiber optic link's swept frequency response at 1.3 μm is characterized with commercially available laser and photodiodes (architecture in Fig. 2(d)). The results are shown in Fig. 5(b) for direct and external modulation schemes. In both cases an InGaAsP laser diode, which has threshold current of 16 mA and cw output power of 3.3 mW at a forward bias current of 50 mA (Ortel 1530A) is used. The laser diode's 3 dB electrical bandwidth is approximately 10 GHz at this same bias point and includes a 45 Ω broadband matching resistor. A 40 GHz bandwidth photodetector (New Focus 1011) is used, whose responsivity is 0.48 mA/mW. It also includes a broadband matching resistance. The length of fiber in all examples is 1 km.

For the externally modulated link, a Mach–Zehnder, Z-cut $LiNbO_3$ EOM with coplanar waveguide electrodes is used. The optical insertion loss is approximately 5 dB and the voltage $V\pi$ for 100% modulation is 5.4 V. Although the link insertion loss is larger than that of the directly modulated link below 12 GHz, it does not experience the characteristic rolloff due to the relaxation oscillation frequency of the laser diode at very high frequencies. Also, as shown in the same figure, increasing on the laser diode increases the directly modulated link bandwidth. However, direct modulation is still limited to microwave frequencies. Thus, the combination of the laser diode for low frequency transmission and the external modulator for millimeter-wave carrier transmission has great potential for realization of fiber optic millimeter-wave subcarrier transmission links.

It should also be pointed out that improvements in the basic link performance can be realized by methods such as impedance matching components, using devices optimized for the particular frequency of interest, and in choosing the operating point of the electrooptic components in terms of bias, input and output powers, etc. The purpose of this work is to demonstrate principles of operation of these link configurations as well as to perform a relative comparison between different two photodetection methods. The results could be significantly improved for certain operating conditions by implementing the above mentioned methods.

Fiber Optic Data Link Performance

In order to demonstrate the principles of millimeter-wave subcarrier transmission over fiber optic links, we configured the link shown in Fig. 3(d) with both 0.83 μm and 1.3 μm optical devices. The fiber optic link's performance is characterized both in terms of digital and analog signal transmissions as shown in the experimental setup in Fig. 6(a). All system impedances are 50 Ω. A bit error rate (BER) measurement is used to characterize both the directly modulated IF link and the externally modulation RF link. An FM analog modulation scheme is also used to evaluate both links. In all measurements, the Tx (transmitter) consists of amplifiers and filters, and where appropriate, an up-converter, all optimized to the frequency in use. The Rcvr. (receiver) contains similar components.

IF Link Evaluation

The IF data portion of the link is first evaluated, using 70 MHz (QPSK) and 300 MHz (FM) subcarriers. The QPSK IF data link portion consists of 1.3 μm optical devices. The clock frequency of QPSK modulator is 6.312 MHz with the IF frequency 70 MHz. The detected IF data signal is amplified and then supplied to the demodulator through the noise and interference measurement test set (HP3708A). The BER performance is shown in Fig. 7(a). A CNR degradation from the theoretical value is within 1.5 dB at an error rate of 10^{-4}. Because the data with the fiber optic link is the same as that without (direct transmission—all electrical), no CNR degradation is caused by the fiber optic link.

The FM IF data link portion is composed of 0.83 μm optical devices and a HEMT detector. The base-bandwidth and required RF bandwidth of the FM modulator are 4.2 MHz and 36 MHz, respectively. Fig 7(b) shows the weighted SNR performance of this IF link versus Ids. The link performances for a MMIC MESFET detector and

(a)
(b)

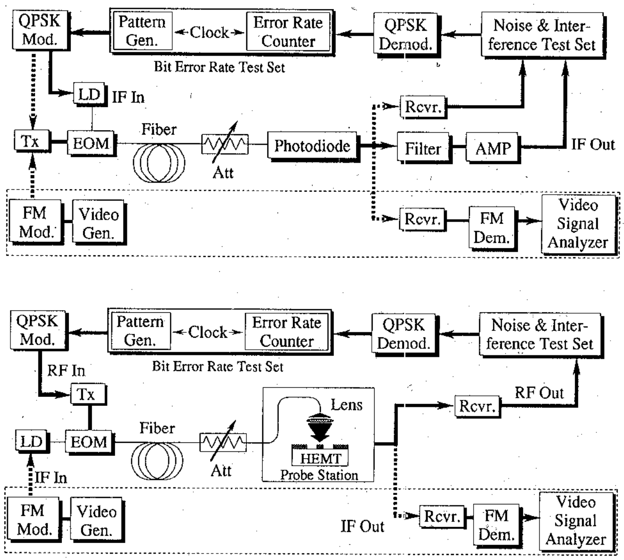

Fig. 6. Experimental configurations for analog and digital signal transmission analysis by fiber optic link. (a) 1.3 μm link configuration of laser diode direct modulation and $LiNbO_3$ external modulation. (b) 0.83 μm HEMT detector evaluation link using modified electrooptic on-wafer probe station.

PIN photodiode are also shown in the same figure for comparison. A weighted SNR of 62.5 dB is achieved by a PIN photodiode. The average weighted SNRs by HEMT and MESFET detectors are about 60 dB and 59 dB, respectively. The difference of the weighted SNR of the HEMT and MESFET detectors arises from the device's transconductance [33]. Although a SNR fluctuation is observed in the experiment due to a large forward current Ids, a high SNR is attained by the MMIC HEMT detector. This fluctuation can be decreased by reducing the input optical power, as shown in Fig. 7(c). In this figure it is shown that as the optical input power is reduced, the magnitude of the SNR fluctuations decrease. It should be noted that at these same frequencies, the HEMT detector has higher responsivity than the PIN photodiode. However, as observed by the SNR, the HEMT noise floor is much higher than that of the PIN photodiode, hence the similar SNRs.

RF Link Evaluation

The RF portion of the fiber optic link is characterized by a 26 GHz subcarrier which transmits either QPSK or FM signals. Availability of the 26 GHz modulators is the primary reason this frequency is used. The $LiNbO_3$ external modulators described in the previous section are also used in this experiment. Ideally, frequencies much higher could be used as long as the external optical modulator met the bandwidth requirement.

The 1.3 μm optical links are evaluated using both digital and analog signals. Fig. 8 shows the BER and weighted SNR performance of links employing a PIN photodiode. The external modulator is modulated by the 26 GHz subcarrier signal. The BER performance is measured using the same QPSK modulator/demodulator as

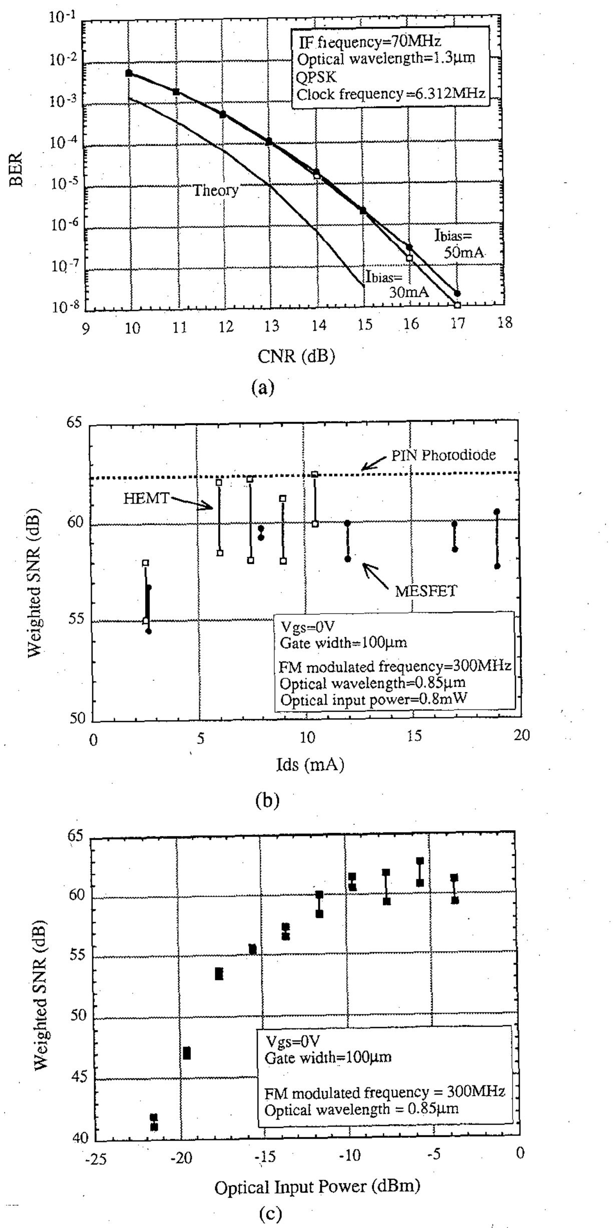

Fig. 7. IF Link performance. (a) QPSK BER results of 1.3 μm, 70 MHz IF link. (b) Weighted SNR results of 0.83 μm, 300 MHz IF link using MMIC HEMT photodetector. (c) Weighted SNR versus optical input power of link in 7(b).

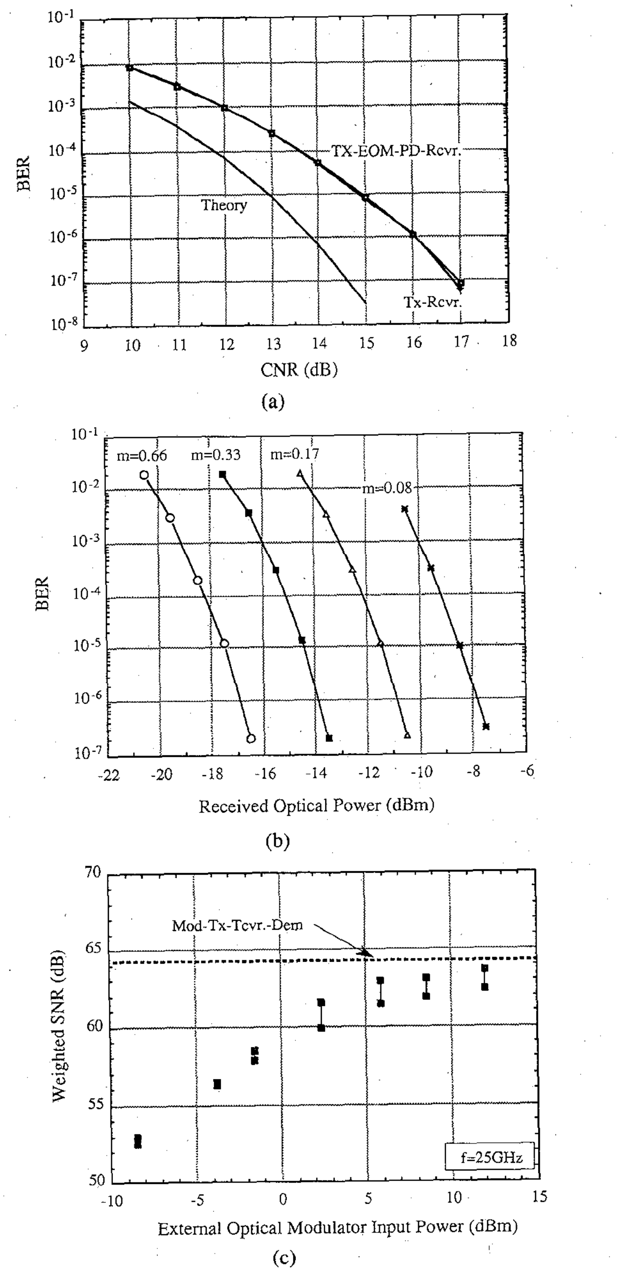

Fig. 8. Link performance of 1.3 μm RF (26 GHz subcarrier) link. (a) BER versus CNR. (b) BER versus received optical input power. (c) Weighted SNR versus modulation input RF power. Dotted line is the weighted SNR without fiber optic link. Maximum and minimum values are represented by black squares.

was used in the IF link. CNR degradation from the theoretical value is within 2 dB and the value is the same as that obtained without the fiber optic link (Tx-Rcvr.), showing no degradation from link insertion. The BER versus the received optical power is shown in Fig. 8(b) for a modulation index of $m = 0.66, 0.33, 0.17$, and 0.08. The modulation index is a function of the subcarrier amplitude and $V\pi$ of the external modulator [34]. The required optical power at the receiver is inversely proportional to the subcarrier input power.

Fig. 8(c) shows the weighted SNR versus the modulation input power (Tx output power). The SNR is first measured by a direct connection of the transmitter (Tx) and receiver (Rcvr.) and then subsequently measured using the fiber optic link inserted. The average weighted SNR of the Tx-Rcvr. link is approximately 64 dB, while that of the fiber optic link is 63 dB at a modulation input power of 12 dBm. The frequency spectrums of the 26 GHz band subcarrier signals are shown in Fig. 8. The QPSK modulated spectrums are shown in Figs. 9 (a) and (b), and the FM modulated spectrums which utilize a standard color bar pattern are shown in Figs. 9(c) and (d). The cause of the amplitude reduction is from the fiber optic link insertion loss. Insertion loss can be overcome pri-

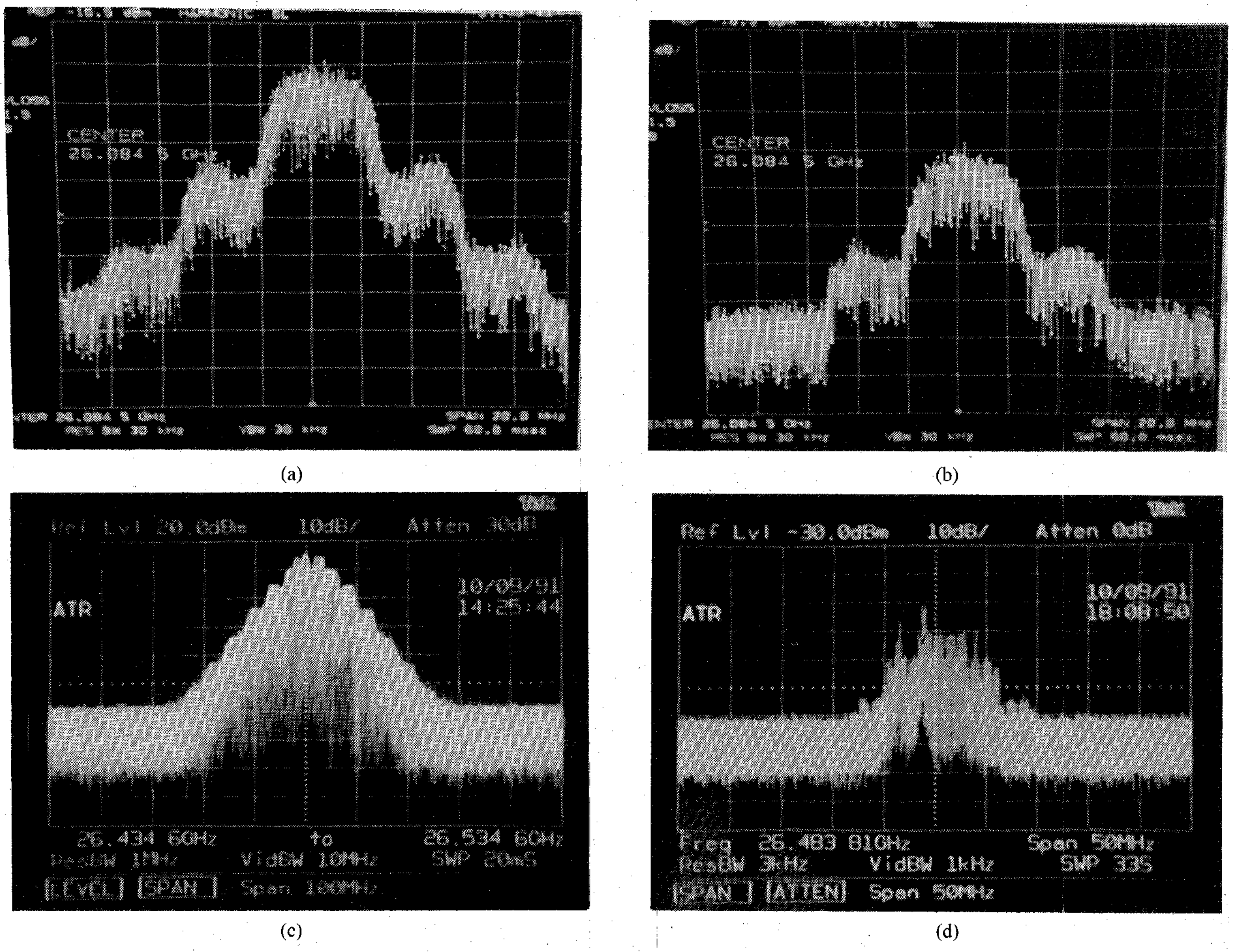

Fig. 9. Frequency spectrums of 26 GHz subcarrier, QPSK and FM modulated, 1.3 μm fiber optic link. (a) Tx QPSK spectrum output. (b) Detected RF QPSK spectrum. (c) Tx FM spectrum output. (d) Detected RF FM spectrum.

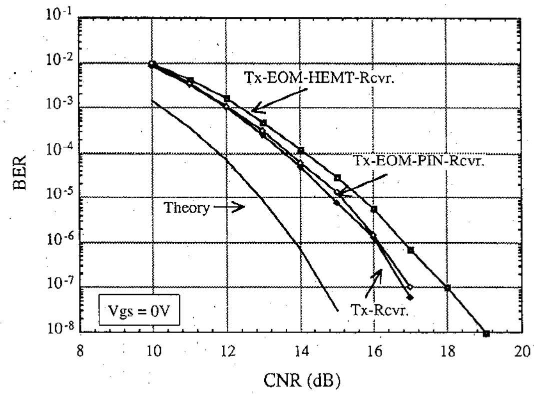

Fig. 10. BER versus CNR performance of 0.83 μm RF (26 GHz subcarrier) link with both HEMT and PIN receivers. The Tx-Rcvr. link has no optical devices.

marily by using a higher power laser diode and optimizing the modulator for operation at the desired frequency.

The RF link composed of HEMT detectors is next characterized with the 26 GHz band subcarrier using the experimental setup shown in Fig. 6(b). The direct Tx-Rcvr. link and the fiber optic link which has a PIN photodiode as a detector are first measured. Next, the link with a HEMT detector is evaluated. The CNR degradation from the PIN photodiode link is less than 0.5 dB and 1 dB at error rates of 10^{-4} and 10^{-8}, respectively as shown in Fig. 10. These results as well as those obtained with the IF link indicate that MMIC HEMT photodetectors are noisier than PIN photodiodes primarily because of the relatively high forward current in the HEMT.

Conclusion

Several fiber optic link configurations for the millimeter-wave subcarrier transmissions are discussed and experimentally investigated. The personal communication system concept which utilizes the above described optical links is also outlined. The combination of direct and external modulation is successfully employed to configure both IF and RF links within the same architecture, and excellent performance of 70 MHz, 300 MHz and 26 GHz subcarrier transmission has been observed.

MMIC HEMT detectors are also introduced for realization of compact and cost-effective optical receivers and are characterized by both digital and analog 26 GHz band subcarriers for the first time. The degradation caused by the insertion of the HEMT fiber optic link is within 2.5 dB from theory. Although the experiments are performed at 26 GHz, the fiber optic links discussed in the this paper can be expected to transmit higher millimeter-wave frequencies by choosing an appropriate external modulator such as a resonant electrode modulator or phase reversal type [35]

Acknowledgment

The authors would like to thank Drs. K. Habara, Y. Furuhama and M. Akaike for their continuous support and encouragement.

References

[1] D. M. Fye, "Design of fiber optic antenna remoting links for cellular radio applications," in *Proc. 40th IEEE Vehicular Technology Conf.*, June 1990, pp. 622–625.

[2] T. S. Chu and M. J. Gans, "Fiber optic microcellular radio," in *Proc. 41st IEEE Vehicular Technology Conf.*, June 1991, pp. 339–344.

[3] R. P. Merrett *et al.*, "A cordless access system using radio-over-fiber techniques," in *Proc. 41st IEEE Vehicular Technology Conf.*, June 1991, pp. 921–924.

[4] C. Harvey *et al.*, "Cordless communications utilizing radio over fiber techniques for the local loop," in *ICC'91 Conf. Rec.*, vol. 3, June 1991, pp. 1171–1176.

[5] M. Shibutani *et al.*, "Feasibility studies on an optical fiber feeder system for microcellular mobile communication systems," in *ICC'91 Conf. Rec.*, vol. 3, June 1991, pp. 1176–1181.

[6] A. J. Cooper, "Fiber-radio: A new technique for delivering cordless access services," in *GLOBECOM'91 Conf. Rec.*, Dec. 1991, pp. 999–1005.

[7] T. E. Darcie *et al.*, "Wide-band lightwave distribution system using subcarrier multiplexing," *J. Lightwave Technol.*, vol. LT-7, pp. 997–1004, June 1989.

[8] R. Olshansky *et al.*, "Subcarrier multiplexed lightwave systems for broadband distribution," *J. Lightwave Technol.*, vol. LT-7, pp. 1329–1341, Sept. 1989.

[9] W. I. Way, "Subcarrier multiplexed lightwave systems design considerations for subscriber loop applications," *J. Lightwave Technol.*, vol. LT-7, pp. 1806–1818, Nov. 1989.

[10] J. M. Chiddix *et al.*, "AM video on fiber in CATV systems: Need and implementation," *J. Lightwave Technol.*, vol. LT-8, pp. 1229–1239, Sept. 1990.

[11] M. Pilgrim and R. P. Searle, "mm-wave direct-to-home multichannel TV delivery system," in *IEEE MTT-S Int. Microwave Symp. Dig.*, June 1989, pp. 1095–1098.

[12] R. D. Carver, "Millimeter-wave radio for broadband local access," in *ICC'91 Conf. Rec.*, vol. 3, pp. 1187–1190, June 1991.

[13] K. B. Bhasin and D. J. Connolly, "Advances in gallium arsenide monolithic microwave integrated-circuit technology for space communications systems," *IEEE Trans. Microwave Theory Tech.*, vol. MTT-34, pp. 994–1001, Oct. 1986.

[14] R. Goyal, *Monolithic Microwave Integrated Circuits.* Norwood, MA: Artech House, 1989.

[15] M. Dagenais et al., "Applications and challenges of OEIC technology: A report on the 1989 Hilton Head Workshop," *J. Lightwave Technol.*, vol. LT-8, pp. 846–861, June 1990.

[16] P. C. Claspy and K. B. Bhasin, "Optical detectors for GaAs MMIC integration: Technology assessment," in *Proc. SPIE, Vol 1102 Optical Technology for Microwave Applications IV*, pp. 53–60, Mar. 1989.

[17] K. A. Dallabetta, "MMIC compatible photodetector design and characterization," in *Proc. SPIE, Vol. 1371 High-Frequency Analog Fiber Optic Systems*, pp. 116–127, Sept. 1990.

[18] A Paolella *et al.*, "Optically controlled GaAs MMIC switch using a MESFET as an optical detector," in *IEEE MTT-S Int. Microwave Symp. Dig.*, May 1990, pp. 941–944.

[19] W. I. Way *et al.*, "A 1.3-μm 35-km fiber-optic microwave multicarrier transmission system for satellite earth station," *J. Lightwave Technol.*, vol. LT-5, pp. 1325–1331, Sept. 1990.

[20] Recommendations and Reports of the CCIR, Rep. 719-2, pp. 167–177, 1986.

[21] A. S. Daryoush *et al.*, "Fiber optic links for millimeter wave communication satellites," in *IEEE MTT-S Int. Microwave Symp. Dig.*, pp. 933–936, May 1988.

[22] D. Donald *et al.*, "Efficient, simple optical heterodyne receiver: DC to 80 GHz," in *Proc. SPIE. Vol. 545, Optical Technology for Microwave Applications II*, pp. 29–34, 1985.

[23] G. J. Simonis and K G. Purchase, "Optical generation, distribution, and control of microwaves using laser heterodyne," *IEEE Trans. Microwave Theory Tech.*, vol. 38, pp. 667–669, May 1990.

[24] T. Sueta and M. Izutsu, "Integrated optic devices for microwave applications," *IEEE Trans. Microwave Theory Tech.*, vol. 38, pp. 477–481, May 1990.

[25] A. S. Daryoush *et al.*, "High-speed fiber-optic links for distribution of satellite traffic," *IEEE Trans. Microwave Theory Tech.*, vol. 38, pp. 510–516, May 1990.

[26] W. E. Stephens and T. R. Joseph, "System characteristics of direct modulated and externally modulated RF fiber-optic links," *J. Lightwave Technol.*, vol. LT-5, pp 380–387, Mar. 1987.

[27] D. Polifko and H. Ogawa, "Fiber optic link architectural comparison for millimeter wave transmission," in *Proc. SPIE, vol. 1703 Microwave Optical and Phased Array Processing*, Apr. 1992.

[28] M. Muraguchi *et al.*, "26 GHz-band full MMIC transmitters and receivers using a uniplanar techniques," in *IEEE MTT-S Int. Microwave Symp. Dig.*, May 1990, pp. 873–876.

[29] J. P. Noad *et al.*, "FET photodetectors: A combined study using optical and electron-beam stimulation," *IEEE Trans. Elect. Dev.*, vol. ED-29, pp. 1792–1797, Nov. 1982.

[30] P. C. Claspy and K. B. Bhasin, "Microwave response of a HEMT photoconductive detector," *Microwave and Optical Technology Lett.*, vol. 2, pp. 1–3, Jan. 1989.

[31] S. Paolella *et al.*, "Optical response of the GaAs MESFET at microwave frequencies and applications," in *IEEE MTT-S Int. Microwave Symp. Dig.*, June 1991, pp. 487–490.

[32] T. Takenaka and H. Ogawa, "An ultra-wideband MMIC balanced frequency doubler using Line-Unified HEMTs," *IEEE Trans. Microwave Theory Tech.*, vol. MTT-40, pp. 1935–1940, Oct. 1992.

[33] R. N. Simons, "Microwave performance of an optically controlled AlGaAs/GaAs high electron mobility transistor and GaAs MESFET," *IEEE Trans. Microwave Theory Tech.*, vol. MTT-35, pp. 1444–1455, Dec. 1987.

[34] A. S. Daryoush *et al.*, "Interfaces for high speed fiber optic link," in *1991 IEEE MTT-S Int. Microwave Symp. Dig.*, June 1991, pp. 297–300.

[35] D. Polifko *et al.*, "Millimeter-wave optical transmission with combination narrowed EOM and laser modulation," in *Proc. Fourth Optoelectronics Conf., OEC'92*, pp. 250–251, July 1992.

[36] K. Hosogi *et al*, "Photo/EB hybrid exposure process for T-shaped gate superlow-noise HEMTs," *Electron Lett.*, vol. 27, no. 22, pp. 2011–2012, Oct. 1991.

Hiroyo Ogawa (M'84), for a photograph and biography, see this issue, p. 2284.

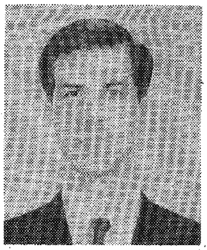

David Polifko (M'91) received the B.S. degree from the University of North Carolina, Charlotte and the M.S. degree from Drexel University, both in electrical engineering, in 1988 and 1991, respectively. Before attending Drexel, he worked at AT&T Bell Laboratories, in the Electronics and Photonics Materials Research Department. Currently he is with ATR Optical and Radio Communications Research Laboratories in Kyoto, Japan, conducting research in the areas of microwave and millimeter-wave fiber optic links for personal communication systems.

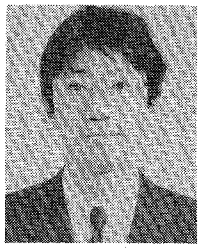

Seiichi Banba received the B.S. and M.S. degrees in electrical engineering from Toyohashi University of Technology, Japan, in 1982 and 1984, respectively. In 1984, he joined the Semiconductor Research Center of SANYO Electric Co. Ltd., Osaka, Japan, where he did research and development work on microwave devices. Since 1990, he has been researching optical/microwave monolithic integrated circuits for personal communication systems at ATR Optical and Radio Communications Research Laboratories in Kyoto, Japan.